THE E835 JET TARGET

D. Allspach, G. Boero, G. Garzoglio, A. Hahn,
C. Kendziora, M. Macrì, M. Marinelli, D. Miller, E. Robutti

The upgrade of the jet target, used by E760, had the following purposes:
a) to **increase** the **density (atoms/cm^3) of the cluster-jet** in the interaction area, by at least a factor two
b) to **improve** the ratio between the cluster-jet target thickness and the total gas thickness along the beam line (jet+background). We define this quantity as the "***Jet target efficiency***" (**JTE**)
c) to **allow control of the gas jet intensity** with a dynamic range of five to ten in order to maintain a constant interaction rate
d) to allow the gas-jet to be **aligned** to intercept the antiproton beam optimally.

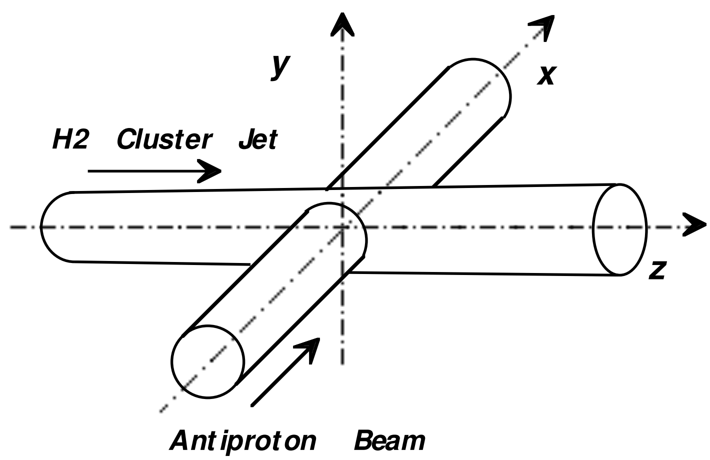

Fig. 1. The antiproton beam-hydrogen cluster-jet interaction area

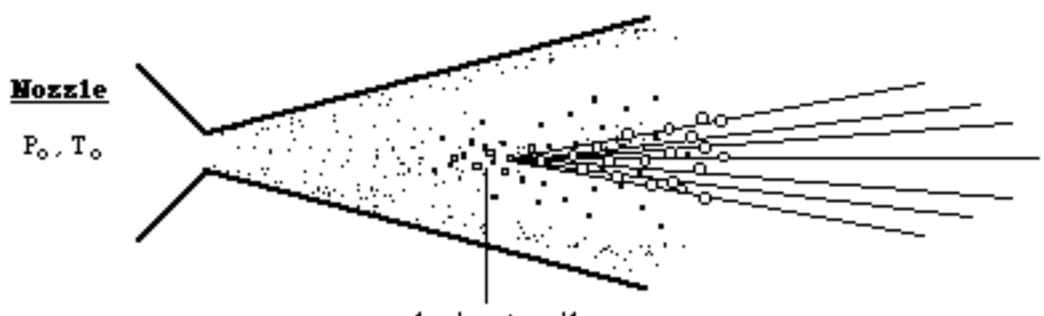

Fig. 2. Condensation and formation of the cluster-jet during gas expansion inside the nozzle.

NOTE: THE MAXIMUM FLOW of HYDROGEN IS 1 milligram/second

The increases in density are achieved by decreasing the stagnation temperature, T_O, of the hydrogen before its expansion through the nozzle throat.

The control of the density is achieved by a system which allows one to set P_O and T_O over a large range and with good precision.

We now have:
1) A new cooling apparatus with its stagnation temperature and pressure control systems

2) Means to control and determine the alignment of the H2 cluster-jet.

3) A LabView based data acquisition and control system.

We have used these to make measurements of the density in the interaction area and of the background gas to obtain the JTE. We have also made measurements to allow a comparison with the performance of the E760 jet target.

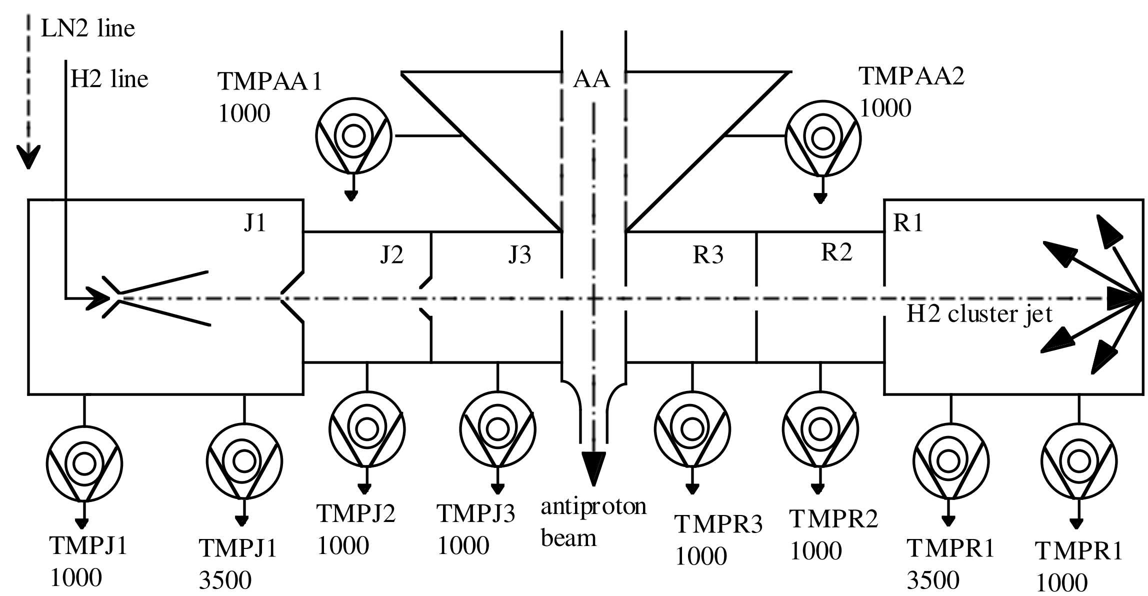

Fig. 3. (*a*) Schematic of the Jet Target with the differential pumping stages: J1, J2, J3: (Jet) production stages; R1, R2, R3: (recovery) sink stages.

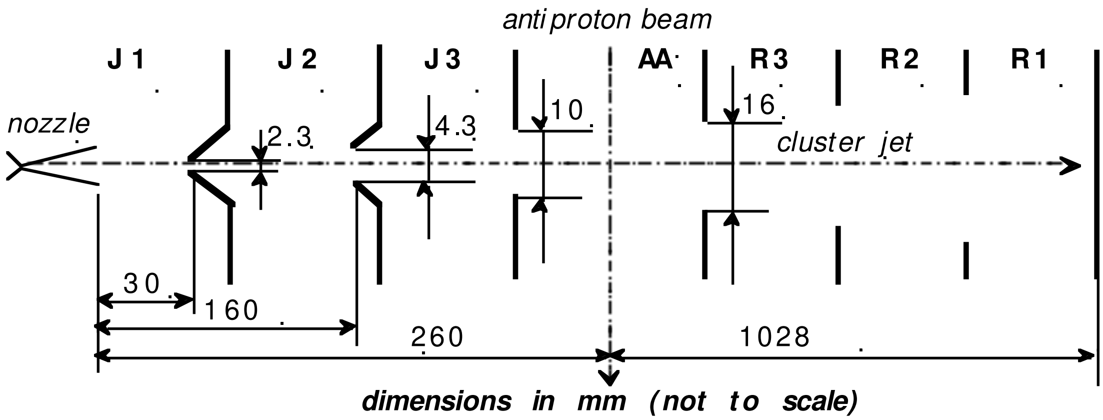

Fig. 3.(*b*) Pertinent Jet target dimensions.

The average density (atoms/cm^3) of the cluster-jet is given by

$$\bar{\rho}_{\text{jet}} = \frac{\Phi_{\text{jet}}}{A_{\text{jet}} v_{\text{cl}}}, \tag{1}$$

Ψ_{jet} is the cluster-jet flux (atoms/s), A_{jet} is the cluster-jet cross section in the interaction area, and v_{cl} is the speed of the clusters.

The experiment luminosity is directly proportional to the product of this density and the current of antiprotons; one wants therefore to maximize Ψ_{jet} and minimize v_{cl}. (Since the cluster-jet has cylindrical symmetry, the quantity A_{jet} is essentially set by the height of the antiproton beam and is not a free parameter).

Lowering the temperature (stagnation temperature T_0) at which the hydrogen expansion begins has both decreased the clusters speed and also produced a substantial improvement in the cluster formation process, thus increasing Ψ_{jet}.

The control of the *x*-*y* position of the nozzle and its angle (fig. 1) optimizes the transmission through the gas-jet collimator and skimmer system.

We have measured Φ_{jet} by calibrating the pumping speeds (S) of the chambers of the gas-jet and using the relation Φ_{jet} = K * S * Pressure

We have measured the cross section by moving a needle through the jet and recording the pressure rise (due to the breakup of clusters) with position.

We have determined the velocity by putting a chopper in the cluster-jet stream and measuring the flight-time over about a meter.

- ***Measurements of Cluster-jet flow and background gas***

The gas *throughput* Q (usually expressed in torr liter/sec, 1 torr liter=3.21 10^{19} molecules @ 300K) inside a chamber can be evaluated knowing the *pumping speed S* and the *pressure P* by means of the relation:

$$Q = S\,P. \tag{2}$$

We obtained the pumping speed on each of the jet target chambers by **introducing a calibrated hydrogen leak flow (i.e., of known throughput) inside each chamber** and measuring the subsequent pressure increase.
We have verified that the method used to introduce the calibrated leak into any chamber allows us to assume that **the pressure increment** produced at the pressure gauge for a given flow rate (number of molecules per unit time) into the chamber **is the same whether the hydrogen is introduced through the calibrated leak or with the cluster-jet stream.**

• ***Measurements of the transverse density distribution of the jet.***

We used a simple method to find the shape of the jet at the interaction region, from which we obtain **the jet cross section** which appears in (1). The method makes use of a thin needle which can travel across the jet, when the hydrogen clusters hit the needle, they break, or "evaporate", scattering individual molecules all around the chamber and causing an increase in pressure. The higher the rate of cluster hits, the larger the pressure rise.

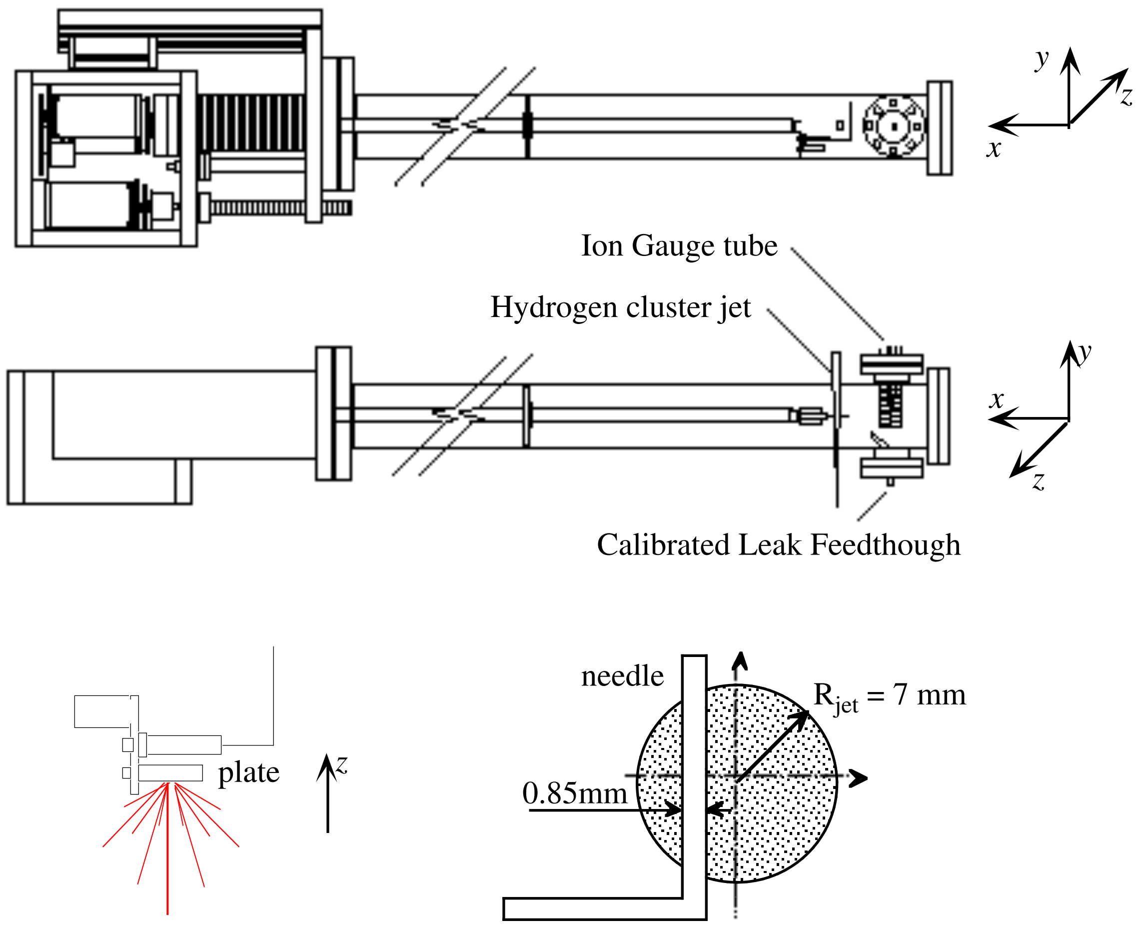

Fig. 4. The *density detector*, used for measuring the geometry and throughput of the cluster-jet.

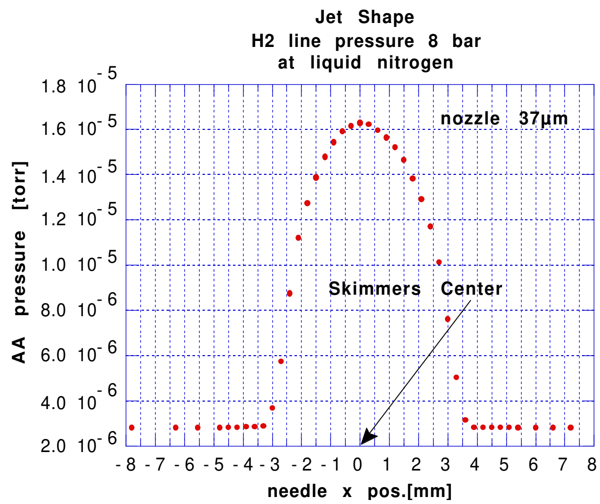

8 (*a*)

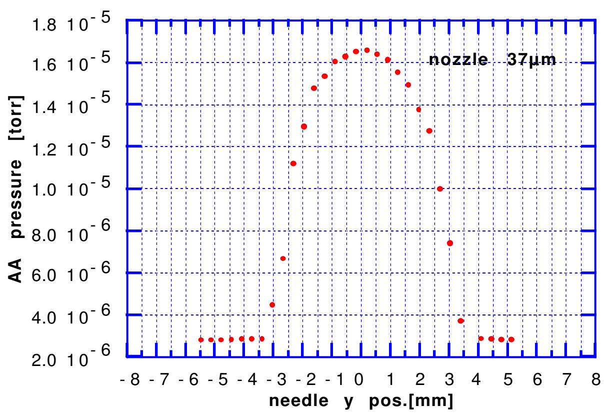

8 (*b*)

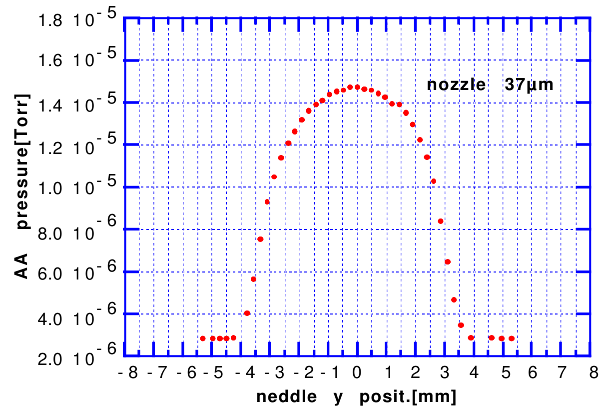

8 (*c*)

Fig. 5. Jet shape plots: *a*) horizontal sweep; *b*) vertical sweep with needle at $z = -19$ mm; *c*) vertical sweep with needle at $z = +19$ mm.

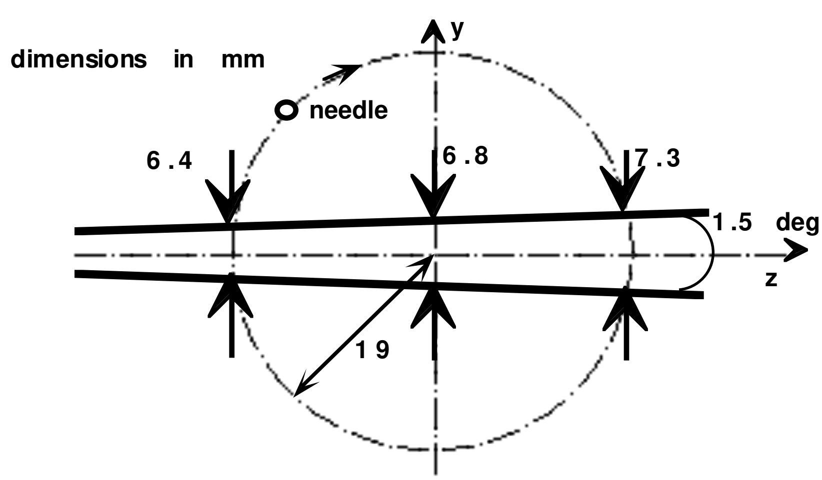

Fig. 6. Jet dimensions inside the Antiproton Accumulator: the 19 mm radius circle swept by the L-shaped needle when rotating around the *x* axis (notice the two intersections with the jet).

The main results of these measurements are: the jet is centered on the x axis to within about 0.5 mm, has a diameter of $(7.0 \pm 0.5)\,\mathrm{mm}$, shows approximately cylindrical symmetry and does not have significant tails (1 mm inside its perimeter the density is more than 80% its maximum).

$$A_{\mathrm{jet}} = (3.85 \pm 0.5) \bullet 10^{-5}\, m^2 \tag{3}$$

- ***Cluster speed***

Another measurement needed for the evaluation of the cluster-jet density is the speed of the clusters. To make this measurement we **periodically chopped the jet inside the Antiproton Accumulator pipe and looked downstream (in the R1 chamber) for the propagation of this perturbation**, thus measuring the elapsed time. The chopper consisted of a rotating metal cylinder with two "quarter period" windows (fig. 7) with its axis along the x direction. Its motor allowed rotation frequencies as high as 400 Hz. The detector was an ion gauge installed in R1 and positioned on the jet stream line.

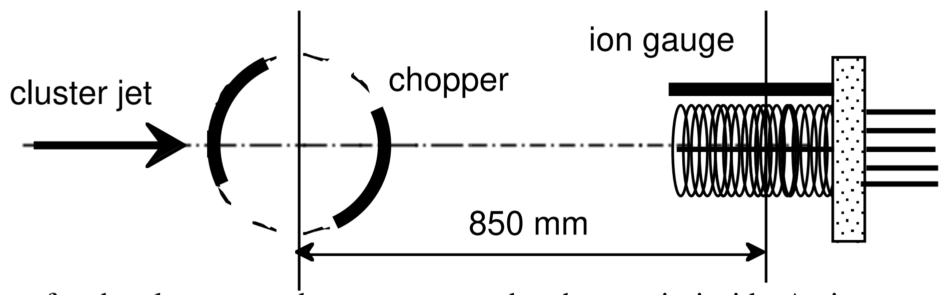

Fig. 7. Set-up for the cluster speed measurement: the chopper is inside Antiproton Accumulator and the detector (a common ion gauge) is inside R1.

We measured the phase difference between the chopper and the signal of the ion gauge with a lock-in amplifier. The trigger comes from a thin slit on the cylinder that periodically passes between a LED and a photo transistor. We have the relation:

$$\Delta\phi = 360 \cdot (2f)t_{of} + c, \tag{4}$$

$\Delta\phi$ is the phase difference between the ion-gauge signal and the chopper, $2f$ is the chopping frequency (twice the motor rotation frequency), t_{of} is the *time of flight*, and c is a constant (frequency independent) offset.

So, we have a linear relation between $\Delta\phi$ and f (fig. 8) and, by repeating the measurement at different values of f, we can extract t_{of} as:

$$t_{of} = \frac{1}{2}\frac{1}{360}\frac{\mathrm{d}(\Delta\phi)}{\mathrm{d}f}. \tag{5}$$

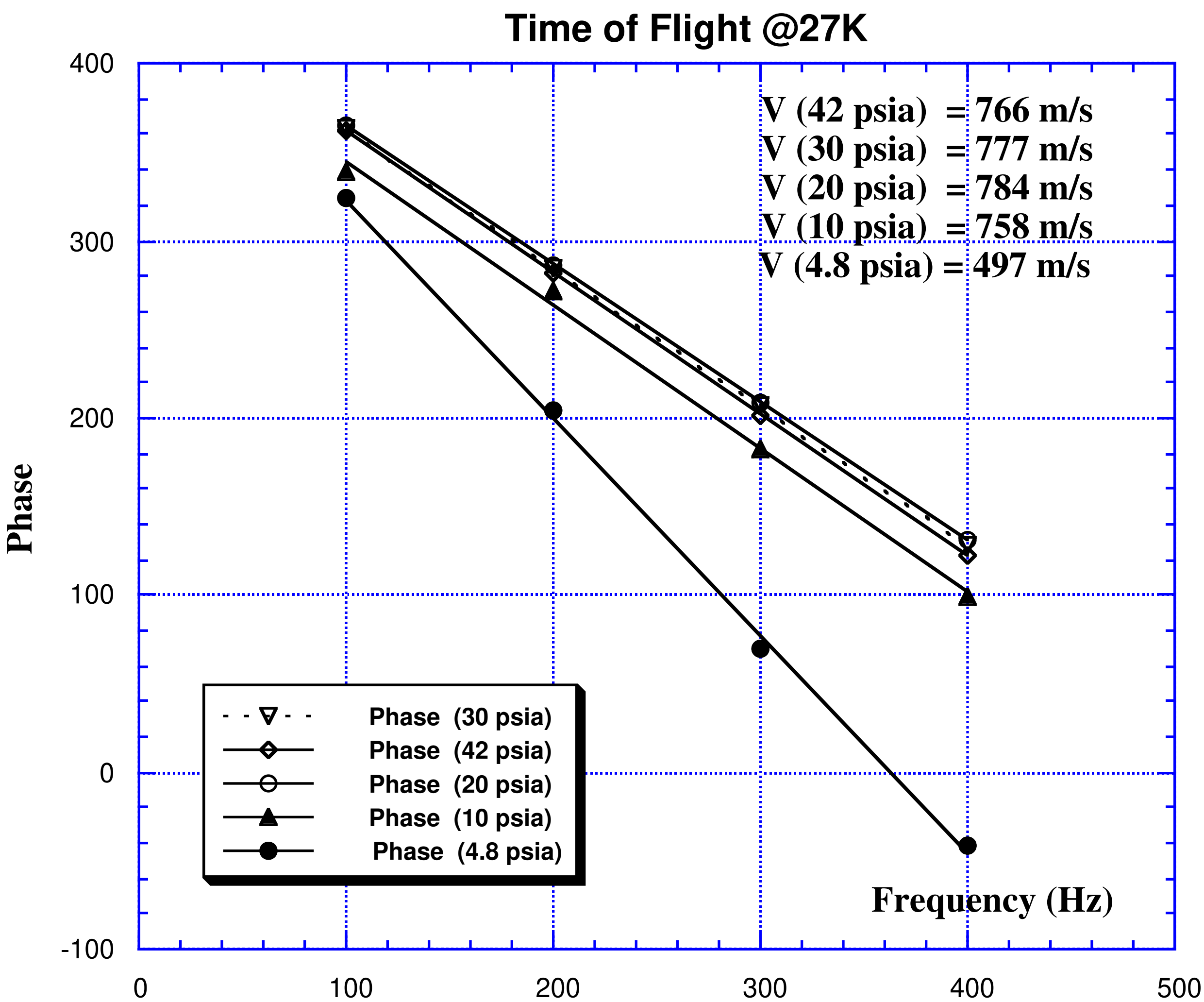

Fig. 8. Phase difference between ion gauge signal and LED/photo transistor signal, as a function of the chopper rotation frequency.

Knowing the distance between the chopper and detector (850 mm) we can obtain v_{cl}.

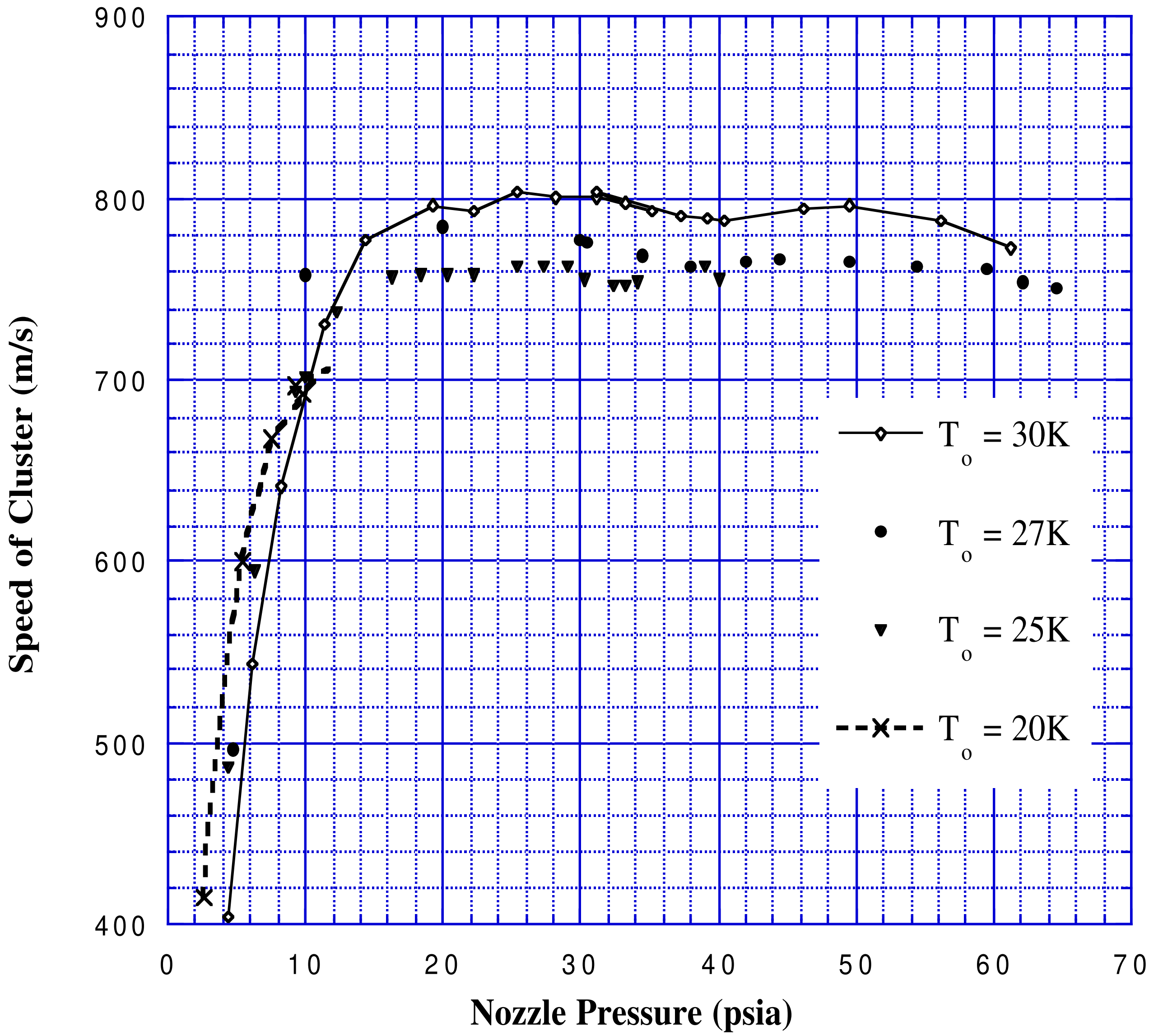

Fig. 9. Examples of speed of the clusters produced by the 37µ nozzle at various temperatures and pressures

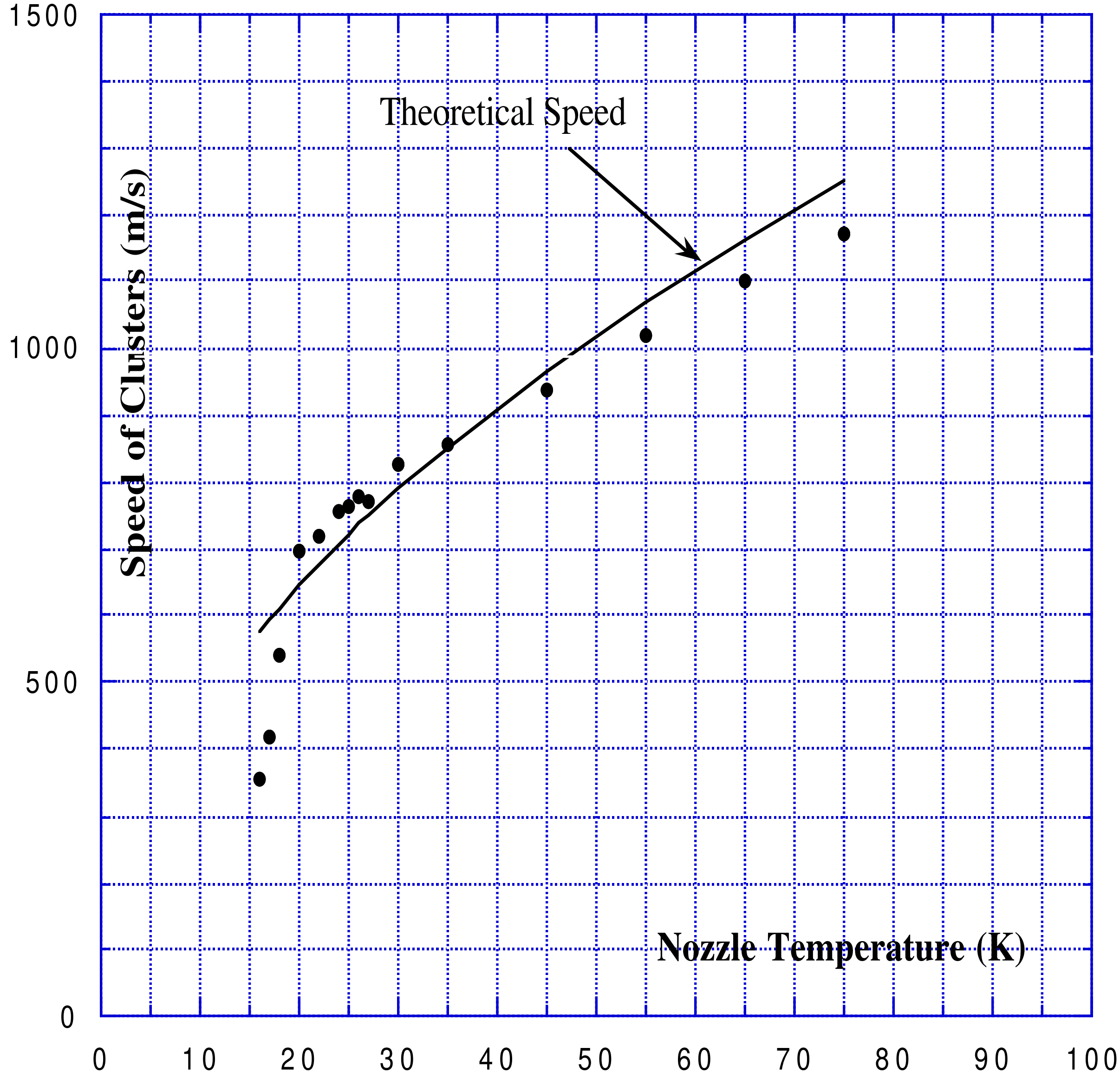

Fig. 10. Speed of the clusters produced by the 37μ nozzle. Comparison between the measured and the theoretical values.

If we treat the expansion as an adiabatic process in a continuum flow regime, we can find an expression for the speed of the clusters:

$$v = \sqrt{\frac{2R}{W}\left(\frac{\gamma}{\gamma-1}\right)T_0} \tag{6}$$

$W = 2.016\ 10^{-3}$ Kg/mole is the weight of a mole hydrogen and $\gamma = c_P / c_V = 5/3$ for molecular hydrogen at low temperature.

• *Results on Gas-jet Density*

Having determined the jet characteristics, we are able to evaluate the cluster-jet average density using equation (1). The nozzle pressure P_o and temperature T_o are not independent variables, thus we choose the $\mathbf{P_o, T_o}$ pair to produce the **right jet density** with a good **JTE**. These points (P_o,T_o) lie in the gas zone of Fig.11 near the phase transition curve.

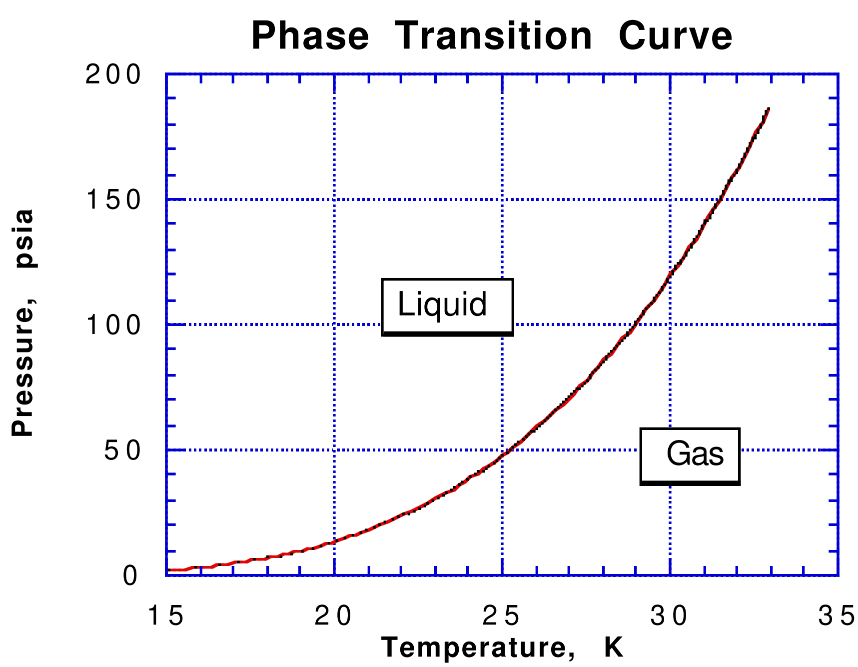

Fig. 11. Phase transition curve for hydrogen. The hydrogen critical point is P_0=186 psia, T_0=33K

Given the upgraded control system, we are able to follow the path of these points which results in the densities and associated JTE's as shown in Fig. 12.

Note that the increase in density is almost a factor of four higher than that achieved in E760.

The JTE has improved from 40% in E760 to almost 90% with the upgraded gas jet. We recall that the JTE is the fraction of gas that gives useful interactions. This improvement is due to the increase in the *cluster fraction* which is the ratio of the number of atoms which clusterize and reach the AA pipe to the total number of atoms which pass through the nozzle. In E760, the cluster fraction was about 3 10^{-3}, whereas now, it is around 20 10^{-3}. Such an effect was anticipated but we did not know how significant it would be.